

Optimized Decimation of Tensor Networks with Super-orthogonalization for Two-Dimensional Quantum Lattice Models

Shi-Ju Ran, Wei Li, Bin Xi, Zhe Zhang and Gang Su*

Theoretical Condensed Matter Physics and Computational Materials Physics Laboratory, School of Physical Sciences, Graduate University of Chinese Academy of Sciences, P. O. Box 4588, Beijing 100049, China

A novel algorithm based on the optimized decimation of tensor networks with super-orthogonalization (ODTNS) that can be applied to simulate efficiently and accurately not only the thermodynamic but also the ground state properties of two-dimensional (2D) quantum lattice models is proposed. By transforming the 2D quantum model into a three-dimensional (3D) closed tensor network (TN) comprised of the tensor product density operator and a 3D brick-wall TN, the free energy of the system can be calculated with the imaginary time evolution, in which the network Tucker decomposition is suggested for the first time to obtain the optimal lower-dimensional approximation on the bond space by transforming the TN into a super-orthogonal form. The efficiency and accuracy of this algorithm are testified, which are fairly comparable with the quantum Monte Carlo calculations. Besides, the present ODTNS scheme can also be applicable to the 2D frustrated quantum spin models with nice efficiency.

PACS numbers: 75.10.Jm, 75.40.Mg, 05.30.-d, 02.70.-c

I. INTRODUCTION

Efficient and accurate numerical methods are very crucial to tackle the strongly correlated quantum lattice systems. To a large class of intriguing correlated electron and spin models, analytical techniques are intractable owing to their extreme complexity and meanwhile, numerical approaches are still challenged by the huge Hilbert space that increases exponentially with the lattice size. Two decades ago, numerical renormalization group algorithms based on density matrix for the ground states¹ and thermodynamic properties² of one-dimensional (1D) systems were proposed, where the thoughtful selection rules were suggested for optimally approximating the Hilbert space with an effective subspace. Very recently, efficient representations with tensor networks as well as the corresponding algorithms for the two-dimensional (2D) quantum models, for instance, the projected entangle pair state (PEPS)³, the tree tensor network⁴, the multiscale entanglement renormalization ansatz state⁵, the infinite PEPS^{6,7}, the tensor renormalization group (TRG)⁸⁻¹⁰, and so on, have been suggested. Some of them already gained interesting applications (e.g. Refs. [11,12]). These algorithms are well testified for calculating the ground state properties, while the algorithms for the thermodynamics of the infinite 2D quantum models still need to be developed.

In this paper, we propose the optimized decimation of tensor networks with super-orthogonalization (ODTNS) to simulate efficiently not only the thermodynamic but also the ground state properties of 2D quantum spin lattice models. Inspired by the projection method of the ground states of 2D systems⁹ and the linearized TRG method for thermodynamic properties of 1D systems¹³, we represent the finite temperature density operator of the 2D quantum model with a three-dimensional (3D) closed tensor network (TN) that consists of the initial tensor product density operator (TPDO) and the 3D brick-wall TN for the evolution along the imaginary time direction. The finite temperature properties can be obtained by linearly contracting the brick-wall TN with the

corresponding imaginary time length to get the TPDO¹³. To bound the dimension of the TPDO, we develop the Tucker decomposition¹⁴ to the TN and propose the network Tucker decomposition (NTD) that transforms a TN into the super-orthogonal form so that an optimal lower-dimensional approximation for the bond space can be reached based on the network singular value spectrum. We testify the efficiency of the ODTNS scheme by calculating the thermodynamic properties of the unfrustrated spin-1/2 Heisenberg antiferromagnet on single-layer and bilayer honeycomb lattices, and the obtained results show the great agreement with quantum Monte Carlo (QMC) calculations. We also calculate the thermodynamic and magnetic properties of the frustrated bilayer model to study the effect of frustration. In what follows, we shall present the procedure of the ODTNS algorithm with a 2D quantum spin system on a honeycomb lattice as a prototype.

II. TENSOR NETWORK REPRESENTATION OF THE FINITE TEMPERATURE DENSITY OPERATOR

In accordance with the general definition of the TN's, we define a TN as a network consisting of the product of tensors (T) and vectors (λ), as shown in Fig. 1. Graphically, a point with some connected bonds represents a tensor; each bond represents an index; a bond that connects two points is called geometrical bond which means a shared index by two tensors that should be contracted; a bond that only connects one point is called the physical bond. We restrict here that one bond must connect one or two points. If an index is shared by more than two tensors (say n), the restriction would always be fulfilled by introducing an n th-order super-diagonal tensor. The points on the geometrical bonds represent vectors. A TN with no physical bonds is called a closed TN [Fig. 1 (a)], e.g. a TN that denotes the partition function of a classical model; a TN with N physical bonds is called an open TN, which contains d^N degrees of freedom (where d is the dimension of one physical bond, Fig. 1 (b)), e.g. a TN that represents a tensor

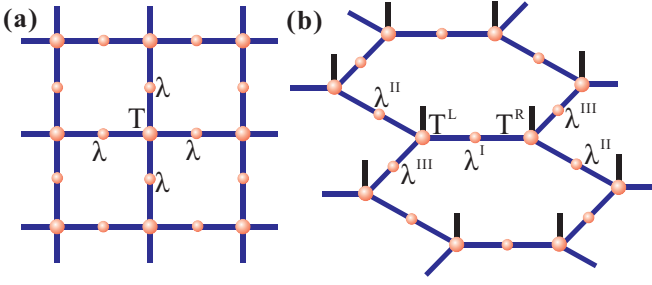


FIG. 1: (Color online) (a) A closed square TN in which each tensor T has four geometrical bonds that connect each other and no physical bond. On each geometrical bond there defines a vector λ . (b) An open honeycomb TN consisting of two inequivalent tensors T^L and T^R , each of which has three geometrical bonds and one physical bond. Three inequivalent vectors λ^I , λ^{II} and λ^{III} are defined on three inequivalent bonds of the TN, respectively.

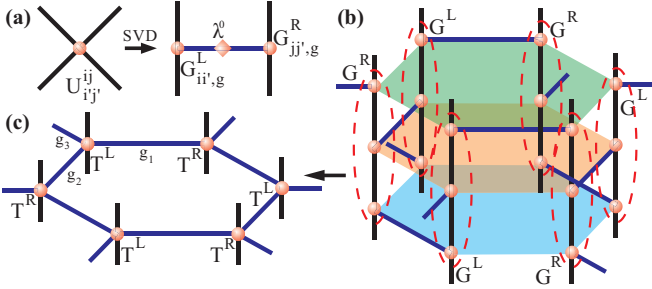


FIG. 2: (Color online) (a) The local evolution operator $U_{i'j'}^{ij}$ is decomposed via an SVD into two gates, $G_{ij,g}^L$ and $G_{i'j',g}^R$, each of which has two physical bonds (i, i' and j, j' , black) and one geometrical bond (g , blue); (b) Contract the shared physical bonds among G^L and G^R to get tensors T^L and T^R ; (c) A TPDO with inverse temperature τ . Note that the singular value vectors $\lambda^{I,II,III}$ on each geometrical bond are not indicated in (b) and (c) for conciseness.

product state or a tensor product operator.

The finite temperature density operator of a 2D system can be transformed into an open TN. Suppose that the Hamiltonian can be written as $H = \sum_{i,j} \hat{H}_{ij}$, where \hat{H}_{ij} is a local Hamiltonian of pairs of spins. The partition function Z is the trace of the density matrix $\rho = \exp(-\beta H)$ with $\beta = 1/T$ the inverse temperature and $k_B = 1$. By means of the Trotter-Suzuki decomposition¹⁵, the density operator can be written as $\rho \approx [\exp(-\tau \sum_{i,j} \hat{H}_{ij})]^{K+1}$, where $\beta = (K+1)\tau$, and τ is the infinitesimal imaginary time slice. Define a local evolution operator $\hat{U}_{ij} = \exp(-\tau \hat{H}_{ij})$. Then, the density operator can be represented as $\rho \approx [\prod_{i,j} \hat{U}_{ij}]^{K+1} = \prod_{q=1}^{K+1} \prod_{i,j} \hat{U}_{ij}^q$, where q is the Trotter index. By making a singular value decomposition (SVD) on $U_{i'j'}^{ij} = \langle ij | \hat{U}_{ij} | i'j' \rangle$ where $|ij\rangle$ stands for the direct product basis of spins at site i and j , we have $U_{i'j'}^{ij} = \sum_g G_{i'j',g}^L \lambda_g^0 G_{ij,g}^R$, where λ^0 is the singular value vector, and G^L and G^R are two local evolution tensors, each of which has two physical bonds (i, i' and j, j' , respectively) and one geometrical bond (g). For a honeycomb lattice, this step is depicted in Figs. 2 (a) and (b).

Next, by contracting the shared bonds among G^L and G^R

[Fig. 2 (b)], we get

$$\begin{aligned} T_{il,g_1g_2g_3}^L &= \sum_{jk} G_{ij,g_1}^L G_{jk,g_2}^L G_{kl,g_3}^L, \\ T_{il,g_1g_2g_3}^R &= \sum_{jk} G_{ij,g_1}^R G_{jk,g_2}^R G_{kl,g_3}^R, \end{aligned} \quad (1)$$

where g_1, g_2 and g_3 are three inequivalent bonds on a honeycomb lattice [Fig. 2 (c)]. The density operator ρ at an inverse temperature τ has the form of a TN as

$$\rho_{\dots i'j'j'j' \dots} = Tr_G(\dots \lambda_{g_2}^{II} \lambda_{g_3}^{III} T_{i'j',g_1g_2g_3}^L \lambda_{g_1}^I T_{jj',g_1g_2g_3}^R \lambda_{g_2}^{II} \lambda_{g_3}^{III} \dots), \quad (2)$$

in which Tr_G is the trace over all contracted geometrical bonds, and $\lambda^I, \lambda^{II}, \lambda^{III}$ are three inequivalent singular value vectors with the initial value λ^0 . This gives a TPDO, which is an extension of the matrix product density operator¹⁶ and the tensor product states. In fact, the TPDO is an open TN comprised of the infinite product of two inequivalent tensors T^L and T^R for two sublattices of the honeycomb lattice as well as λ^I, λ^{II} and λ^{III} for three inequivalent bonds [Fig. 2 (c)]. The TPDO at finite temperature consists of two parts: the initial TPDO and the 3D brick-wall structure formed by the product of evolution tensors. We can contract linearly the evolution tensors in pairs into the TPDO along the imaginary time direction. For example for bond g_1 , we have

$$\begin{aligned} \tilde{T}_{ik,(g_1g'_1)g_2g_3}^L &= \sum_j G_{ij,g'_1}^L T_{jk,g_1g_2g_3}^L, \\ \tilde{T}_{ik,(g_1g'_1)g_2g_3}^R &= \sum_j G_{ij,g'_1}^R T_{jk,g_1g_2g_3}^R, \end{aligned} \quad (3)$$

and meanwhile, we get $\tilde{\lambda}_{g_1g'_1}^I = \lambda_{g_1}^0 \lambda_{g'_1}^I$. The contractions for bonds g_2 and g_3 are similar. After certain times of contraction, we obtain the TPDO at the corresponding inverse temperature. Then by tracing all bonds, we can get the partition function Z at finite temperature. During the contraction, as the dimension of the geometrical bonds is unavoidably enlarged, an optimal approximation is needed to bound the bond dimension. In the existing algorithms for truncating the bond, a matrix SVD on the matricization of the tensor is used and the states with D_c (dimension cut-off) largest singular values are preserved. We extend the Tucker decomposition to the TN's and suggest the NTD to transform the TN into a super-orthogonal form, with which the optimal approximation can be obtained with the robust network singular value spectrum (NSS).

III. SUPER-ORTHOGONAL FORM OF TENSOR NETWORKS AND NETWORK TUCKER DECOMPOSITION

In the areas of data compression, image processing, etc., Tucker decomposition has been accepted as a convincing higher-order generalization of matrix singular value decomposition, and its approximation scheme for a single tensor has wide and successful applications¹⁷. It can be written as the product of the form

$$T_{i_1 i_2 \dots i_n} = \sum_{j_1 j_2 \dots j_n} S_{j_1 j_2 \dots j_n} U_{i_1 j_1}^{(1)} U_{i_2 j_2}^{(2)} \dots U_{i_n j_n}^{(n)}. \quad (4)$$

The tensor S is called the core tensor and $U_{i_k j_k}^{(k)}$ is the unitary matrix. This decomposition is considered as a higher-order generalization of the matrix SVD when the core tensor S satisfies the following two conditions:

(a) All-orthogonal: $\sum_{i_1 i_2 \dots i_{\alpha-1} i_{\alpha+1} \dots i_n} S_{i_1 i_2 \dots i_{\alpha} \dots i_n} S_{i_1 i_2 \dots i'_{\alpha} \dots i_n} = 0$ if $i_{\alpha} \neq i'_{\alpha}$ for any α ;

(b) Ordering: $\|S_{i_{\alpha}=1}\| \geq \|S_{i_{\alpha}=2}\| \geq \dots \geq \|S_{i_{\alpha}=I_n}\|$, where I_n is the dimension of the index i_n , and the norm of the sub-tensor $\|S_{i_{\alpha}=k}\| = \sum_{i_1 i_2 \dots i_{\alpha-1} i_{\alpha+1} \dots i_n} S_{i_1 i_2 \dots i_{\alpha-1} k i_{\alpha+1} \dots i_n} S_{i_1 i_2 \dots i_{\alpha-1} k i_{\alpha+1} \dots i_n}^*$.

All-orthogonality requires that each slice (that means fixing one index when setting others as one composite index free) of the core tensor S is mutually orthogonal with respect to the scalar product of matrices. The ordering condition guarantees that the norm of each sub-tensors of S does not increase as the corresponding index increases, which is similar to the order of matrix singular values. Actually, $\|S_{i_{\alpha}}\|$ is the singular values of the matrix $M_{j i_{\alpha}} = T_{i_1 i_2 \dots i_{\alpha} \dots i_n}$ where the composite index $j = (i_1 i_2 \dots i_{\alpha-1} i_{\alpha+1} \dots i_n)$.

In the Tucker decomposition, the information of the weight is stored in the core tensor, and more specifically, it is the norm of each sub-tensor of S . The optimal lower-dimensional approximation of a single tensor can thus be obtained by keeping the space corresponding to the sub-tensors with larger norms. Several algorithms of the Tucker decomposition have been proposed, such as the higher-order orthogonal iteration in which the interplay among all bonds of the tensor is considered for the optimal approximation.

In the following, we extend the definition and the approximation scheme of the Tucker decomposition for a single tensor to a TN. First we define the network reduced matrix (NRM) \mathcal{M} of bond g_i for a (real) tensor T as

$$\mathcal{M}_{g_i g'_i} = \sum_p \sum_{g_1 g_2 \dots g_n} T_{p, g_1 g_2 \dots g_i \dots g_n} T_{p, g_1 g_2 \dots g'_i \dots g_n} (\lambda_{g_1} \lambda_{g_2} \dots \lambda_{g_{i-1}} \lambda_{g_{i+1}} \dots \lambda_{g_n})^2 \lambda_{g_i} \lambda_{g'_i}, \quad (5)$$

where $p = \{p_1, p_2, \dots, p_m\}$ denotes the composite bond of all physical indices because one can always rearrange all physical indices into a composite index, g_i denotes a geometrical bond, and $T_{p, g_1 g_2 \dots g_i \dots g_n}$ represents an element of the tensor T . The super-orthogonal form of an open TN is defined by two conditions:

(a) Ordering: all λ 's on geometrical bonds are positive-defined, normalized and the elements of each λ are in descending order. We coin the vectors λ 's as the network singular value spectrum, that is a generalization of the matrix singular value spectrum.

(b) Orthogonality: for any tensor T in the TN and any geometrical index g_i of T , the NRM \mathcal{M} is diagonal and equals to the square of the corresponding λ , say $\mathcal{M}_{g_i g'_i} = \lambda_{g_i}^2 \delta_{g_i g'_i}$.

The super-orthogonal conditions, which are non-local, require that the matrix $A_{(p g_1 g_2 \dots g_{i-1} g_{i+1} \dots g_n), g_i} = T_{p, g_1 g_2 \dots g_n} \lambda_{g_1} \lambda_{g_2} \dots \lambda_{g_{i-1}} \lambda_{g_{i+1}} \dots \lambda_{g_n}$ (that is analog to the singular vectors of matrix SVD) is column orthogonal for any i . These conditions are global constraints for the TN, as every tensor should satisfy them simultaneously. From the NSS which contains the information of the weight distribution instead of the core tensor in the Tucker decomposition, the

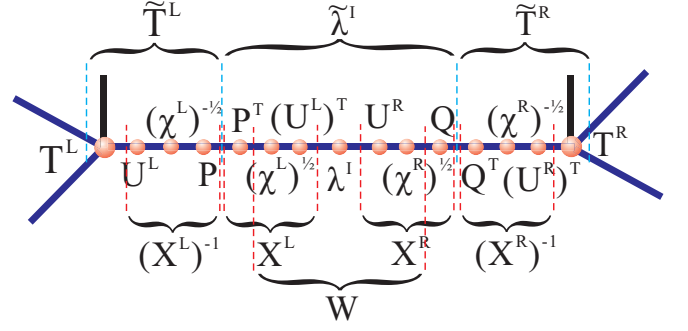


FIG. 3: (Color online) The identical transformation within the NTD for the bond g_1 of an open honeycomb TN.

optimal low-dimensional approximation of the bond space can be obtained. For 1D systems, the super-orthogonal conditions require that the matrix product states (MPS)'s satisfy simultaneously the left and right canonical conditions defined in Ref. [18], which leads to the canonical form of MPS.

Within the suggested NTD, the super-orthogonal form is gained by iteratively transforming the TN with identical transformations on each geometrical bond until the pre-established convergence to the super-orthogonal form is reached. For instance, for bond g_1 (Fig. 3) the transformation matrices X^L and X^R for T^L and T^R (the transformation matrices Y^L and Y^R for bond g_2 , Z^L and Z^R for bond g_3 are similar) are defined by

$$\begin{aligned} X_{ab}^L &= \sum_c P_{ca} (\chi_c^L)^{-1/2} U_{bc}^L, \\ X_{ab}^R &= \sum_c Q_{ca} (\chi_c^R)^{-1/2} U_{bc}^R, \end{aligned} \quad (6)$$

where $U_{bc}^{L(R)}$ contains eigenvectors and $\chi_c^{L(R)}$ contains the eigenvalues of the matrix $\bar{M}_{bc}^{L(R)} = (\lambda_b^L \lambda_c^L)^{-1} \mathcal{M}_{bc}^{L(R)}$. P (Q) contains the left (right) singular vectors of the intermediate matrix W defined by

$$W_{ac} = \sum_b (\chi_b^L)^{1/2} U_{ba}^L \lambda_b^L U_{bc}^R (\chi_c^R)^{1/2} \stackrel{\text{svd}}{=} \sum_g P_{ag} \tilde{\lambda}_g^I Q_{bg}. \quad (7)$$

By inserting the identity $I = X^L (X^L)^{-1} = X^R (X^R)^{-1}$ into the left (right) side of λ^I and transforming T^L , T^R and λ^I , we have

$$\tilde{T}_{p, gbc}^L = \sum_a T_{p, abc}^L (X^L)_{ag}^{-1}, \quad \tilde{T}_{p, gbc}^R = \sum_a T_{p, abc}^R (X^R)_{ag}^{-1}, \quad (8)$$

$$\tilde{\lambda}_g^I \delta_{gg'} = \sum_a X_{ga}^L \lambda_a^I X_{ag'}^R = \sum_{af} P_{ag} W_{af} Q_{fg'}. \quad (9)$$

With new \tilde{T}^L , \tilde{T}^R and $\tilde{\lambda}^I$ as well as λ^{II} and λ^{III} , the NRM of the bond g_1 equals to $(\tilde{\lambda}^I)^2$ as the matrices $\bar{A}_{p, abc}^{L(R)} = \sum_{a'} T_{p, a' bc}^{L(R)} \lambda_b^{II} \lambda_c^{III} U_{a'a}^{L(R)} (\chi_a^{L(R)})^{-1/2}$ and $P(Q)$ are both column orthogonal and normalized.

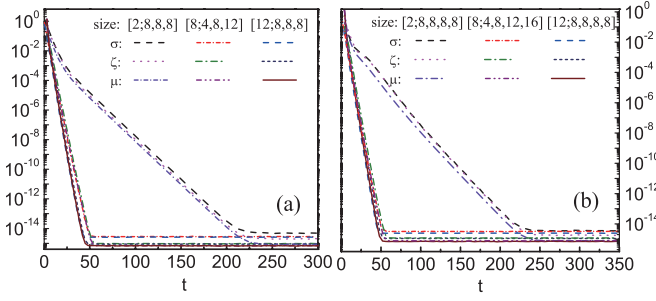


FIG. 4: (Color online) The convergence of μ , σ and ζ of open (a) honeycomb and (b) square TN's with the increase of the iteration step t . $[D_p; D_{g_1}, D_{g_2}, \dots, D_{g_n}]$ is the size of the tensors that form the TN, where D_{g_i} ($i = 1, 2, \dots, n$) is the dimension of the geometrical bonds and D_p is the dimension of the physical bond. Each factor is obtained from the average of the results of 100 randomly initialized TN's. The error of the eigenvalue decomposition ζ is about 10^{-15} .

After doing similar transformations on the other two bonds, \bar{A} bears the form of

$$\begin{aligned} \bar{A}_{p,abc}^{L(R)} &= \sum_{a'} \bar{T}_{p,a'bc}^{L(R)} \bar{\lambda}_b^{II} \bar{\lambda}_c^{III} U_{a'a}^{L(R)} (\chi^{L(R)})_a^{-1/2} \\ &= \sum_{a'b'c'} T_{p,a'b'c'}^{L(R)} (\lambda_{b'}^{II} \gamma_{b'b}^{R(L)}) (\lambda_c^{III} z_{c'c}^{R(L)}) U_{a'a}^{L(R)} (\chi^{L(R)})_a^{-1/2}. \end{aligned} \quad (10)$$

It can be seen from Eqs. (6) and (10) that the super-orthogonal conditions are satisfied when the eigenvalues $\chi^{L(R)}$ in Eq. (6) are uniformly distributed (i.e., all eigenvalues are equal to 1) for all three bonds. The deviation of $\chi^{L(R)}$ from uniform distribution can be measured by $\zeta = (|\chi^L - \mathcal{V}| + |\chi^R - \mathcal{V}|)/(2\mathcal{L})$, in which $|\bullet|$ means the norm of a vector, \mathcal{V} is a vector with all its elements equal to 1 and \mathcal{L} is the length of the vector χ . In addition, we define a factor that measures the convergence of λ 's at the t th iteration by $\mu(t) = \sum_{S=I,II,III} (|\lambda^S(t-3) - \lambda^S(t)|/|\lambda^S(t)|)/3$, and a factor $\sigma = (\sigma^L + \sigma^R)/2$, where $\sigma^{L(R)} = \sum_{ab} |\mathcal{M}_{ab}^{L(R)} - (\lambda_a^S)^2 \delta_{ab}|$ measures TN's deviation from the super-orthogonal form according directly to the super-orthogonal conditions.

To testify the robustness of the super-diagonal form and the efficiency of NTD, we randomly initialize the inequivalent tensors and vectors (according to Gaussian distribution $N(0, 1)$) that form the infinite open honeycomb and square TN, and calculate the factors μ , σ and ζ with different iteration steps. The value of each factor is the average of the results of 100 randomly initialized TN's. Fig. 4 shows that the NTD can transform a randomly initialized TN into a super-orthogonal form very efficiently. It is found that ζ and σ decay exponentially to about $10^{-14} \sim 10^{-15}$ (where the error of the eigenvalue decomposition itself ζ is about 10^{-15}) within 300 steps. Meanwhile, μ converges to $10^{-14} \sim 10^{-15}$, which justifies the good convergence of the three inequivalent λ 's. We may see that for a certain TN, the three factors share one same super-orthogonalization ratio ξ and in general, ξ becomes larger when we increase the space of the physical bond and fix the space of the geometrical bonds.

The computational cost to transform a TN into the super-

orthogonal form with NTD is mainly from the eigenvalue (singular value) decompositions of $D_g \times D_g$ matrices, which is about $O(tD_g^3)$ with t the transformation steps and D_g the dimension of the geometrical bond. In the ODTNS scheme, the TPDO converges to the super-orthogonal form with $\sigma < 10^{-8}$ only with $t \sim 10$ steps, because for a small τ , the evolution is nearly identical.

IV. THE FREE ENERGY

After each time that the evolution tensors are contracted into the TPDO, we super-orthogonalize the TPDO and obtain the optimal approximation of the enlarged geometrical bonds as well as the λ^S 's ($S = I, II, III$). By collecting the normalization factor $r_q^S = \sqrt{\sum_g \lambda_g^S}$ with q the Trotter step, the free energy per site can be obtained with r_q^S and \bar{r}^{19} that is the contraction of the TPDO by

$$f(\beta) = \frac{1}{2\beta} \left(\sum_{q=1}^K \sum_{S=I,II,III} \ln r_q^S + 2 \ln \bar{r} \right). \quad (11)$$

The thermodynamic quantities of the 2D quantum lattice systems can be obtained from the free energy $f(\beta)$.

What is more, the ground state properties can also be obtained with the ODTNS scheme. When one takes $K \rightarrow \infty$ and $\tau \rightarrow 0$, the ground state energy per site e_0 has a simple form of

$$e_0 = \lim_{K \rightarrow \infty} \lim_{\tau \rightarrow 0} \frac{1}{2\tau} \ln \prod_{S=I,II,III} r^S. \quad (12)$$

V. THERMODYNAMICS OF SPIN-1/2 ANTIFERROMAGNET ON A HONEYCOMB LATTICE

To judge the efficiency and accuracy of the ODTNS algorithm, let us consider the spin-1/2 antiferromagnet on an infinite honeycomb lattice with $\hat{H}_{ij} = \delta(\hat{S}_i^x \hat{S}_j^x + \hat{S}_i^y \hat{S}_j^y) + \hat{S}_i^z \hat{S}_j^z$, where δ measures the anisotropy of spin interactions. In following calculations, μ is kept smaller than 10^{-820} , and the lattice size for QMC calculations is 64×64 .

Fig. 5 shows the energy difference $\Delta E = |E - E_{QMC}|$ between the results obtained by ODTNS and QMC calculations at different inverse temperature β in the absence of the magnetic field, where $\tau = 10^{-2}$ and $D_c = 30$. We find that, when $\delta = 0.5$, there exists a thermodynamic phase transition, and the energy difference is about $10^{-4} \sim 10^{-5}$ at both high and low β . Near the critical point the difference is relatively high but is still smaller than 0.003. When $\delta = 1$, the system is gapless, and the energy difference is about 10^{-3} at both high and low β , and near the crossover point, the difference is also relatively high but still remains around 10^{-2} . These results show that the precision of ODTNS scheme is comparable with that of QMC.

We investigated ΔE versus the dimension cut-off D_c near the critical (crossover) β , as shown in Fig. 6, where $\tau = 10^{-2}$.

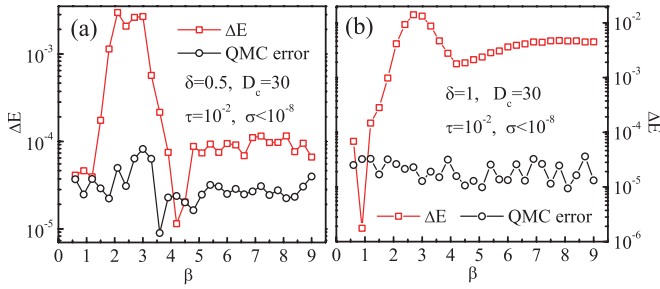


FIG. 5: (Color online) The energy difference $\Delta E = |E - E_{QMC}|$ between the ODTNS and QMC calculations and the QMC error at different inverse temperature β for the spin-1/2 Heisenberg antiferromagnet on a honeycomb lattice. (a) shows the result at $\delta = 0.5$ when the system suffers a thermodynamic phase transition; (b) shows the result at $\delta = 1$ when the system is gapless and a thermodynamic phase transition is forbidden by Mermin-Wagner theorem. We set $\tau = 10^{-2}$, $\sigma < 10^{-8}$ and $D_c = 30$.

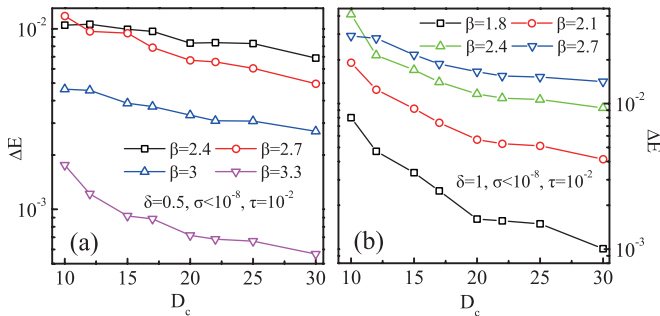


FIG. 6: (Color online) The energy difference $\Delta E = |E - E_{QMC}|$ between ODTNS and QMC with the dimension cut-off D_c near the critical (crossover) point for (a) $\delta = 0.5$ and (b) $\delta = 1$. It can be seen that ΔE becomes smaller as D_c is increased. The QMC error is around 10^{-5} .

It is observed that the energy difference becomes smaller when D_c is increased. When β is away from the critical (crossover) point, we uncovered that different D_c gives errors within 10^{-4} . We also checked ΔE for different τ , and disclosed the (Trotter) errors are within 10^{-4} .

The specific heat as a function of β is calculated by $C = -\beta^2 dE/d\beta$, as shown in Fig. 7 for $\delta = 0.5$. A divergent peak at a critical temperature T_c is observed, which indicates that a phase transition occurs between a paramagnetic phase and an antiferromagnetic phase at T_c . Such a phase transition is also confirmed with the result of the staggered magnetization, shown in the inset of Fig. 7. The QMC results are also included for a comparison. One may see that both results from the ODTNS and QMC calculations agree quite well, showing again the efficiency and accuracy of the present method. In addition, the present ODTNS algorithm can be directly applied to the 2D frustrated quantum spin models.

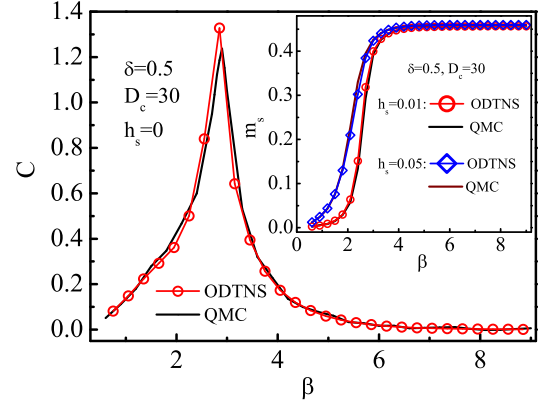


FIG. 7: (Color online) The inverse temperature β dependence of the specific heat at $\delta = 0.5$ and $h_s = 0$ for the spin-1/2 anisotropic Heisenberg antiferromagnet on a honeycomb lattice. The QMC result with the error around 10^{-3} is included for a comparison. The inset shows the staggered magnetization at the magnetic field $h_s = 0.01$ and 0.05 , and the QMC error is around 10^{-5} .

VI. THERMODYNAMICS OF A SPIN-1/2 FRUSTRATED BILAYER HONEYCOMB HEISENBERG MODEL

We apply the ODTNS algorithm to explore the spin-1/2 Heisenberg model on a bilayer honeycomb lattice with the Hamiltonian $\hat{H} = \sum_{\langle ij \rangle} \hat{H}_{ij}$, where $\hat{H}_{ij} = \hat{H}_{ij}^{(1)} + \hat{H}_{ij}^{(2)} + (\hat{H}_i^{(a)} + \hat{H}_j^{(b)})/3$, $\hat{H}_{ij}^{(1,2)} = J_{1,2}[\delta_{1,2}(\hat{S}_i^x \hat{S}_j^x + \hat{S}_i^y \hat{S}_j^y) + \hat{S}_i^z \hat{S}_j^z]$ the anisotropic Heisenberg antiferromagnet on each layer and $\hat{H}_i^{(a,b)} = J_{a,b}[\delta_{a,b}(\hat{S}_i^x \hat{S}_j^x + \hat{S}_i^y \hat{S}_j^y) + \hat{S}_i^z \hat{S}_j^z]$ the interlayer coupling [see the inset of Fig. 8 (a) for the layout of the model], $\delta_{1,2}$ and $\delta_{a,b}$ measure the corresponding anisotropy of nearest neighbor spin interactions. We take $J_1 = J_2 = 1$ as energy scale.

When both J_a and J_b are positive, the couplings are all antiferromagnetic, and the system has no frustration. The energies obtained by the ODTNS algorithm at $J' = J_a = J_b = 1$ and 3 are shown in Fig. 8 (a), which are in good agreement with QMC results (where the QMC error is within 10^{-5}).

When J_a and J_b take different signs, the system becomes frustrated and the QMC simulations fail because of suffering from the negative sign problem. Fig. 8 (b) shows the results of energy and specific heat at $J' = J_a = -J_b = 1$ and 3 . When $J' = J_a = 1$, a second-order phase transition is found at $\beta_c = 2.75(5)$; when $J' = 3$, no phase transition is observed from the specific heat. Notice that the frustration reaches the maximum at $J' = 3$ in the Ising limit for this present model. Fig. 9 presents the sublattice magnetization per site m_s at $J' = 1$ and 3 where the frustration exists. At $J' = 1$, the couplings within each layer are dominant. The system is in the antiferromagnetic phase at low temperature and there exists a thermal phase transition from the antiferromagnetic to paramagnetic phase. At $J' = 3$ when the strong frustration is present, m_s is around 10^{-3} , indicating the absence of magnetic long range order at all temperature. These calculations

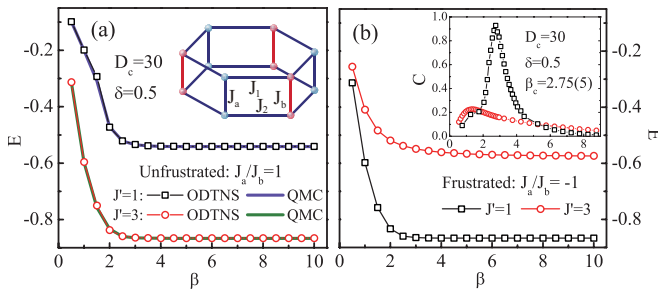


FIG. 8: (Color online) The inverse temperature β dependence of the energy for the spin-1/2 Heisenberg model on a bilayer honeycomb lattice for (a) $J' = J_a = J_b = 1$ and 3, and (b) $J' = J_a = -J_b = 1$ and 3. The inset of (a) shows the bilayer structure of the system and the inset of (b) shows the specific heat C of the 2D frustrated quantum spin system.

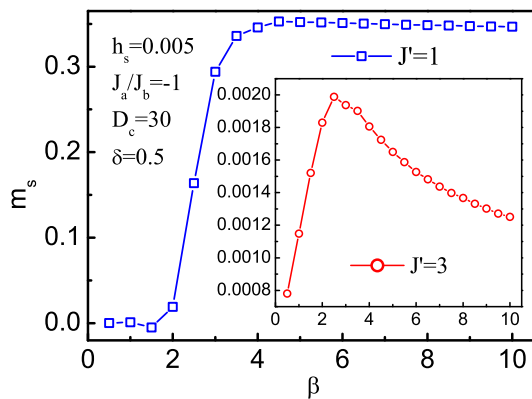


FIG. 9: (Color online) The sublattice magnetization per site m_s , at $J' = J_a = 1$ and 3 (inset) for the spin-1/2 frustrated Heisenberg model on a bilayer honeycomb lattice, where $J_a/J_b = -1$.

show that the ODTNS algorithm is capable of studying the 2D frustrated quantum spin systems.

VII. SUMMARY

In summary, a novel algorithm based on the ODTNS scheme for the 2D quantum spin lattice models is proposed. By mapping the 2D quantum model into a 3D TN, we suggest the NTD to obtain the optimal approximation of the bond space by transforming the TPDO into the super-orthogonal form, that leads to an efficient and accurate calculation of the free energy as well as other observables in the 2D quantum systems. We testify the efficiency and accuracy of the present algorithm by studying the thermodynamics of a spin-1/2 Heisenberg antiferromagnet on a honeycomb lattice, and compare the results with those of the QMC. It is shown that the precision of the ODTNS algorithm is comparable with that of the QMC as both results agree very well. In addition, we find that the present algorithm can also be applied to explore the 2D frustrated quantum spin models without suffering from a negative-sign problem. It is expected that the present ODTNS scheme could also be extended to 2D correlated electron systems.

Acknowledgments

The authors are indebted to J. Chen, X. Yan, F. Ye, Y. Zhao and Q. R. Zheng for stimulating discussions. This work is supported in part by the NSFC (Grant Nos. 90922033 and 10934008), the MOST of China (Grant No. 2012CB932901) and the CAS.

* Corresponding author. Email: gsu@gucas.ac.cn

¹ S. R. White, Phys. Rev. Lett. **69**, 2863 (1992), Phys. Rev. B **48**, 10345 (1993).

² R. J. Bursill, T. Xiang, and G. A. Gehring, J. Phys. Condens. Matter **8**, L583 (1996); X. Q. Wang and T. Xiang, Phys. Rev. B **56**, 5061 (1997).

³ F. Verstraete and J. I. Cirac, arXiv:cond-mat/0407066; J. Jordan, R. Orús, G. Vidal, F. Verstraete, and J. I. Cirac, Phys. Rev. Lett. **101**, 250602 (2008).

⁴ Y.-Y. Shi, L.-M. Duan, and G. Vidal, Phys. Rev. A **74**, 022320 (2006); L. Tagliacozzo, G. Evenbly, and G. Vidal, Phys. Rev. B **80**, 235127 (2009).

⁵ G. Vidal, Phys. Rev. Lett. **99**, 220405 (2007); Phys. Rev. Lett. **101**, 110501 (2008).

⁶ H. C. Jiang, Z. Y. Weng, and T. Xiang, Phys. Rev. Lett. **101**, 090603 (2008).

⁷ L. Wang and Frank Verstraete, arXiv:cond-mat/1110.4362v1.

⁸ M. Levin and C. P. Nave, Phys. Rev. Lett. **99**, 120601 (2007).

⁹ Z. Y. Xie, H. C. Jiang, Q. N. Chen, Z. Y. Weng, and T. Xiang, Phys. Rev. Lett. **103**, 160601 (2009).

¹⁰ Z. C. Gu, M. Levin, and X. G. Wen, Phys. Rev. B **78**, 205116 (2008); Z.C. Gu and X. G. Wen, Phys. Rev. B **80**, 155131 (2009).

¹¹ P. Chen, C. Y. Lai, and M. F. Yang, J. Stat. Mech. P10001 (2009).

¹² W. Li, S. S. Gong, Y. Zhao, and G. Su, Phys. Rev. B **81**, 184427 (2010); W. Li, S. S. Gong, Y. Zhao, S. J. Ran, S. Gao, and G. Su, Phys. Rev. B **82**, 134434 (2010); X. Yan, W. Li, Y. Zhao, S. J. Ran, and G. Su, Phys. Rev. B **85**, 134425 (2012).

¹³ W. Li, S. J. Ran, S. S. Gong, Y. Zhao, B. Xi, F. Ye, and G. Su, Phys. Rev. Lett. **106**, 127202 (2011).

¹⁴ L. De Lathauwer, B. De Moor, and J. Vandewalle, SIAM. J. Matrix Anal. and Appl. **21**, 1324-1342 (2000).

¹⁵ M. Suzuki and M. Inoue, Prog. Theor. Phys. **78**, 787 (1987); M. Inoue and M. Suzuki, Prog. Theor. Phys. **79**, 645 (1988).

¹⁶ F. Verstraete, J. J. Garca-Ripoll, and J. I. Cirac, Phys. Rev. Lett. **93**, 207204 (2004).

¹⁷ See T. G. Kolda and B. W. Bader, SIAM Rev. **51**, (3) (2009), etc.

¹⁸ R. Orús and G. Vidal, Phys. Rev. B **78**, 155117 (2008).

¹⁹ We contract the TPDO by first tracing the physical bonds to obtain an infinite 2D closed TN and then contracting this TN with the ODTNS algorithm.

²⁰ Note that without the iteration in the NTD, σ is on the same order of τ for the imaginary time evolution, which could lead to the results unstable near the critical (crossover) point. If one reduces τ to decrease σ without making iterations in the NTD, the cost

would be very high because the extremely large evolution steps are needed to reach a certain temperature.